- 1 "Orbital control of Pleistocene euxinia in Lake Magadi, Kenya"
- 2 D.M. Deocampo¹, R.B. Owen², T.K. Lowenstein³, R.W. Renaut⁴, N.M. Rabideaux⁵, A.
- 3 Billingsley⁶, A. Cohen⁷, A.L. Deino⁸, M.J. Sier^{9,10}, S. Luo¹¹, C.-C. Shen^{12,13}, D. Gebregiorgis¹, C.
- 4 Campisano¹⁴, A. Mbuthia¹⁵
- 5 ¹ Dept. of Geosciences, Georgia State Univ., Atlanta, GA 30302, USA
- 6 ² Dept. of Geography, Hong Kong Baptist Univ., Kowloon Tong, Hong Kong
- 8 ⁴ Dept. of Geological Sciences, Univ.of Saskatchewan, Saskatoon, SK S7N 5E2, Canada
- 9 ⁵ Dept. of Chemistry, Rutgers Univ., Newark, NJ 07102, USA
- 10 ⁶ Dept. of Earth and Atmospheric Sciences, Univ.of Houston, Houston, TX, USA
- 11 ⁷ Dept. of Geosciences, Univ. of Arizona, Tucson, AZ 85721, USA
- 12 ⁸ Berkeley Geochronology Center, 2455 Ridge Road, Berkeley CA 94709 USA
- 13 ⁹ CENIEH, Paseo Sierra de Atapuerca 3, 09002 Burgos, Spain
- 14 Dept. of Earth Sciences, Univ. of Oxford, South Parks Road, OX1 3AN Oxford, United Kingdom
- 15 ¹¹ Dept. of Earth Sciences, National Cheng-Kung University, 701 Tainan, Taiwan, ROC
- 16 ¹² High-Precision Mass Spectrometry and Environment Change Laboratory, Dept. of Geosciences,
- 17 National Taiwan Univ., 10617 Taipei, Taiwan, ROC
- 18 ¹³ Research Center for Future Earth, National Taiwan Univ., 10617 Taipei, Taiwan, ROC
- 19 ¹⁴ School of Human Evolution and Social Change, Institute of Human Origins, Arizona State
- 20 Univ., Tempe, AZ 85287, USA
- 21 ¹⁵ Tata Chemicals Magadi LTD, Box 1-00205, Magadi, Kenya

ABSTRACT

Lake Magadi is an internally-drained, saline and alkaline terminal sump in the southern Kenya Rift. Geochemistry of samples from a ~200-m core representing the past ~1 Myr of the lake's history show some of the highest concentrations of transition metals and metalloids ever reported from lacustrine sediment, including redox-sensitive elements Mo, As, and V. Elevated concentrations of these elements represent times when the lake's hypolimnion was euxinic – that is, anoxic, saline, and sulfide-rich. Euxinia was common over the past ~700 ka, tending to occur during intervals of high orbital eccentricity. These were likely times when high frequency hydrologic changes favored repeated episodes of euxinia and sulfide precipitation. High-amplitude environmental fluctuations at peak eccentricity likely impacted water balance in terrestrial habitats and resource availability for early hominins. These are associated with important events in human evolution, including the first appearance of Middle Stone Age technology between about 500 and 320 ka in the southern Kenya Rift.

INTRODUCTION

The Hominin Sites and Paleolakes Drilling Project (HSPDP) drilled cores in several rift basins of eastern Africa to obtain long, continuous paleoenvironmental records close to important fossil and archaeological sites (Cohen et al., 2016; Campisano et al., 2017). Lake Magadi (Figure 1) is within 100 km of several important sites for human origins research, including Olduvai Gorge, Laetoli, and Peninj, with Olorgesailie <20 km distant. Monsoon intensity fluctuations due to orbital and other factors are hypothesized to have influenced early hominin habitat structure, selective pressures, and speciation (Potts and Faith, 2015). Results from Core HSPDP-MAG14-2A, Olorgesailie outcrops, and Core ODP-OLO12-1A in the Koora Graben (Figure 1), suggest that environmental variability, especially the intensity of arid episodes, between ~500 and 300 ka played a role in mammal species turnover and the first appearance of Middle Stone Age technology (Owen et al., 2018a; 2019; Potts et al., 2018; 2020). Paleolimnological records from the regional drainage sump can offer unique perspectives on environmental change and the timing and drivers of human evolution.

GEOLOGIC SETTING

Lake Magadi occupies a set of subparallel grabens in the rift between metamorphic highlands to the east and west. Magadi Trachyte (~1.4-0.8 Ma) covers much of the rift floor, cut by rift-parallel faulting. Plio-Pleistocene volcanos are found throughout the region, mostly trachyandesitic to basaltic, with a few carbonatites (Baker and Mitchell, 1976).

Lake Magadi is a saline, alkaline ephemeral lake fed by hydrothermal groundwater and ephemeral streams (Jones et al., 1977). It was part of a large Pleistocene paleolake extending

south to Lake Natron (Hillaire-Marcel and Casanova, 1987). Inflow waters are Na-CO₃ brines, with evaporation producing some of the most concentrated alkaline fluids on earth (Deocampo and Jones, 2014). With pH>10, authigenic silicates such as zeolites and magadiite (Na-silicate) are common (Eugster, 1967). Despite hypersaline modern conditions, some Middle to late Pleistocene deposits represent much fresher conditions, including diatomaceous mud with fish fossils (Owen et al., 2018b).

METHODS

Core HSPDP-MAG14-2A was drilled to a depth of 194 m and halted in basal trachyte. Lithologies including dm-scale interbedded resistant chert and soft muds made drilling difficult; total recovery was approximately 60% (Campisano et al., 2017). A Bayesian geochronology was based on radiocarbon, 40 Ar/ 39 Ar, paleomagnetic, and U-series dates using Bacon v.2.2 (Owen et al., 2018a). 344 samples were collected every ~30 cm from intact core segments at the National Lacustrine Core Facility, and analyzed by ICP-MS following a four-acid digestion by ACTLABS (Toronto; Hu and Qi, 2014). Mineralogy was determined with a Panalytical XRD, analyzing randomly oriented powders from 5–65° 20 at 45mV and 40mA (Rabideaux, 2018).

RESULTS

The top ~60 m of core are dominated by trona and trona-bearing zeolitic mud (Cohen et al., 2016). The remainder of the core is mostly laminated to massive zeolitic mud, interbedded with chert. Some intervals contain silt- to sand-sized euhedral cubic pyrite crystals.

Sediments older than ~700 ka have Zr/TiO₂ = ~100, whereas younger sediments have ~2200, with increased variability in bedded trona in the upper part of the core (Figure 2). Zr/TiO₂ ratios reflect source rock geochemistry and are generally unaffected by weathering, so this implies little change in the composition of detrital sources for the basin after the shift ~700 ka. Many samples have Mo (up to 1500 mg/kg), As (up to 200 mg/kg), and V (up to 450 mg/kg) concentrations among the highest ever reported in lacustrine sediments (e.g. Owen et al., 2018b). These transition metals and metalloids are often associated with euxinic sulfide deposits such as pyrite that scavenge them from saline bottom waters (Vorlicek et al., 2004; Thiam et al., 2014). Variable concentrations of Mo, As, and V are found throughout the clays and silts, which are generally dark-colored and reduced; high concentrations are found preferentially in lithologies containing coarse grained pyrite (Figure 2; Sup. Table 1). La/Lu in the core increases from the start of the record at ~1 Ma to ~600 ka, after which La/Lu strongly correlates with Mo, particularly during peak eccentricity intervals (Sup. Tab. 3), with a possible long-term declining trend.

DISCUSSION

Very high concentrations of Mo, As, and V have not previously been observed in East Africa, though high levels are reported in Lake Kivu hot springs (Degens and Kulbicki, 1973).

Owen et al. (2018b) found Mo concentrations above typical ICP-MS detection limits (2 mg/kg) to be rare among hundreds of samples across the region. High Mo, As, and V generally require euxinia: anoxic, sulfide-rich brine. High salinity can occur due to saline hydrothermal input, evaporative concentration, or both; an anoxic hypolimnion in Lake Magadi implies persistent

chemostratification. Shallow saline lakes may be anoxic because dense brines resist wind shear, have low O_2 solubility, and rapidly consume oxygen when warmed (Deocampo and Jones, 2014; De Cort et al., 2019). Therefore, it is not unexpected that mixing and oxygenation only occur during flooding events (Talling, 1992). Freshening, lake level rise, and oxygenation are also supported by bioturbated magadiite beds (~25-9 ka) overlain by muds (Buatois et al., 2020). If lake level rise persists, eventually meromixis may occur, restoring stratification, perhaps with a freshwater cap.

A range of environmental conditions is represented geochemically: well-mixed, well-stratified, and euxinia (Figure 3). Euxinia is likely triggered during negative water balance episodes; complete desiccation is not implied, however, because sulfide precipitation persists. This is consistent with a lack of paleosols in the core (Muiruri et al., 2021), though some cherts show evidence of subaerial exposure (Leet et al., 2021). Hypolimnic euxinia could persist into episodes of lake level rise, as dense bottom waters lie beneath fresher surface waters – perhaps even until thorough mixing occurs. Stratification may be enhanced by lake deepening, but it is not required; for example, shallow water anoxia (<0.1mg/L O₂) is observed at nearby Nasikie Engida with <2 m water depth (De Cort et al., 2019).

Geochemical cyclicity is observed after ~820 ka (Figure 4). Intervals in which Mo >1 σ above the mean co-occur with maximum eccentricity over the past ~700 ka, suggesting sensitivity due to hydrologic closure. Before ~700 ka, the geochemical record was likely not sensitive to paleohydrology and the lake may have been hydrologically open. Nearly constant Zr/TiO₂ before and after ~700 ka suggests a shift in detrital source at that time, likely related to volcanic, tectonic, or geomorphic events (e.g. stream capture or fault movements).

Correlation between La/Lu and Mo after ~600 ka suggests that light rare earth element (LREE) enrichment was highest during euxinia. This is consistent with marine observations where anoxic brines become LREE-enriched due to redox cycling of Mn- and Fe-oxides (Bau et al., 1997). Late Pleistocene Magadi cherts (Kerrich et al., 2002) have an order of magnitude lower La/Lu, suggesting they formed in less euxinic conditions, perhaps even in oxygenated waters. The high La/Lu and Mo values in the uppermost part of the core dominated by evaporite trona reflect the most recent euxinia in the lake over the past ~100kyr, possibly related to basin tectonics rather than climatic forcing (Owen et al., 2019).

Mo and eccentricity have no correlation over the dataset as a whole, but significant correlations (p<0.01) were found in 50 kyr and 100 kyr windows across most of the dataset (Supp. Table 2). Euxinia tends to peak during eccentricity maxima, associated with eccentricity-driven aspects of global paleoclimate records, including sapropel and benthic foraminiferal δ^{18} O records from the eastern Mediterranean (Emeis et al., 2000; Konijnendijk et al., 2014), and the record of glacial terminations over the past 700 ka (Figure 4). Euxinia as indicated by peak Mo concentrations was high at all glacial terminations or shortly thereafter, except Term. V, which fell during an eccentricity minimum when precession forcing was weakest (Supp. Figure 1). Significant cyclicity in the 100 kyr band is observed for the record from ~820 ka to ~200 ka (Figure 4).

High-frequency hydroclimatic changes are known from across eastern Africa during this time interval. At nearby Olorgesailie, shifts between lacustrine and subaerial conditions occur throughout the record over thousands of years (Owen et al., 2008; Deocampo et al., 2010). High-frequency episodic desiccation was shown in the Koora Graben core, ~11 km east of

Magadi (Potts et al., 2020). High-frequency change is also known from Lake Malawi to the south (Lyons et al., 2015; Ivory et al., 2016) and Chew Bahir to the north (Foerster et al., 2018).

Diatom flora in the upper part of the core show high-frequency flood events (Owen et al., 2018a; 2019) and pollen taxa show frequent expansion and contraction of *Podocarpus* forests (Muiruri et al., 2021). These are not represented geochemically likely because dense, euxinic waters can persist long beyond the onset of euxinia, extending even into early diagenesis (Domagalski et al., 1990), and so may not be specifically tied to surface hydrology on short time scales. Absent an oxidizing event such as lake overturning, euxinia indicators could then be time-averaged, smoothing the signal. Accumulation may continue even as a freshwater cap develops, only subsiding upon depletion of the brine, or mixing of the water column.

100 kyr cyclicity in the euxinia signal therefore suggests that intervals of high eccentricity were times when episodes of euxinia were favored, driven by intervals of negative water balance, even as lake level rose and fell. In the diatomaceous upper part of the core, Owen et al. (2018) found high frequency pulses of freshwater benthic taxa representing flood events. While they occurred at higher frequencies, and are not restricted to high-eccentricity times, they occurred more often during high eccentricity intervals, and they correlate with diatom-inferred lake transgressions in the Koora core (Figure 4; Potts et al. 2020).

Euxinia indicators, then, are associated with both aridity and flooding - high amplitude salinity events occurring over precessional or other high frequency timescales, even though the signal may be smoothed out. The greater amplitude of such events during eccentricity maxima argue for an orbital source of the variability (i.e. precession), as the amplitude of precession is itself modulated by eccentricity over the Pleistocene (Berger and Loutre, 1994). When the

amplitude of precession was weakest during low eccentricity (e.g. ~400 ka), Mo is correspondingly low, suggesting breakdown in euxinia (Figure 4). High Mo at the beginning of this low eccentricity interval may represent a lag after the eccentricity peak ~495 ka.

High amplitude (i.e. precession-scale) environmental fluctuations undoubtedly had a profound impact on moisture availability and vegetation over evolutionary timescales (Potts, 2013). This likely influenced habitats for early hominins and other vertebrates, vertebrate faunal turnover, expansion of early hominin material transport range, and the development of Middle Stone Age technologies (Potts et al., 2018; 2020).

CONCLUSIONS

Drilling in the Lake Magadi basin and geochemical analyses have yielded lake sediments with some of the highest Mo, As, and V concentrations ever reported. These indicate euxinia, strong stratification with anoxic, sulfidic, and saline hypolimnic waters, beginning at ~700 ka. Before then, the basin likely was not sensitive to orbitally induced changes in regional hydrology, and perhaps was not even hydrologically closed. At ~700 ka, a significant event occurred that changed the sediment source and made the lake hydrologically sensitive. REE data suggest a gradual increase in anoxia from ~700–450 ka, after which eccentricity-scale variability dominates. Peaks in euxinia indicators (Mo, As, V) tended to occur during intervals of high eccentricity and are associated with most glacial terminations over the past 700 ka.

The Lake Magadi geochemical record adds to the body of evidence emphasizing the importance of eccentricity modulation of precession in Pleistocene records of hydroclimate in eastern Africa. It also provides a clear indicator of intense droughts in the region during glacial

maxima since ~700 ka, superimposed on a long-term increase in aridity known from other proxy records. Euxinia episodes in Lake Magadi are consistent with environmental fluctuations hypothesized to play a role in vertebrate and human evolution and the emergence of the Middle Stone Age in East Africa.

ACKNOWLEDGEMENTS

HSPDP was funded by the ICDP and US-NSF (EAR-1123942, BCS-1241859, BCS-1241790, EAR-1322017, EAR-1338553, and 1349599) and the Hong Kong Research Grants Council. U-series dating was supported by grants of the Ministry of Education and Ministry of Science and Technology of Taiwan ROC and National Taiwan University. We thank the National Museums of Kenya, the Kenyan National Council for Science and Technology, the Kenyan Ministry of Mines, the National Environmental Management Authority of Kenya, Tata Chemicals, and Magadi County Council for permissions. DOSECC Exploration Services provided drilling support and the National Lacustrine Core Facility assisted in drilling, core description, sampling, and core curation. Three anonymous reviewers are thanked for their helpful reviews. This is HSPDP publication #42.

FIGURE CAPTIONS

Figure 1. Location and stratigraphy of Core MAG14-2A. A: Topography of the south Kenya Rift, view toward the west (GeomappApp.org). B: View north over Lake Magadi (June 2019) showing trona rafts and seasonally flooded lake. C: Bayesian chronological model for Core MAG14-2A.

See Owen et al., 2018a. D. Simplified lithological log.

Figure 2. Trace metal geochemistry of core MAG14-2A, calculated as running 5-point averages. A shift in Zr/TiO_2 ratios suggests basin reorganization at ~700 kyr, and otherwise fairly constant source area geochemistry. La/Lu ratios suggest a gradual increase in anoxia up until ~600 kyr, after which it is cyclical, correlating with euxinia indicators Mo, As, and V.

Figure 3. Model of euxinia indicator accumulation in Lake Magadi. (A) Well-mixed waters preserve only traces of Mo, As, and V especially during lake level rise, as these elements sorb or precipitate easily. (B) stratified waters accumulate significant concentrations as sustained anoxia mobilizes these elements into the aqueous phase. (C) hyperaccumulation in sulfide phases (i.e. pyrite) as extreme evaporative concentration and anoxia combine to raise concentrations in anoxic bottom waters.

Figure 4. Paleoclimate context of Lake Magadi euxinia. Mo shows 100 kyr cyclicity after ~820 ka, with peaks occurring in high eccentricity intervals, associated with the last eight glacial terminations, and the Mediterranean benthic foraminiferal and sapropel records (Emeis et al., 2000; Konijnendijk et al., 2014). Diatom assemblages suggesting flood events are found at a much higher frequency, and may occur more frequently during interglacials, though not exclusively (Owen et al., 2018a). Insolation curve from Laskar et al. (2004). Mo wavelet shows power in the 100 kyr band, with cone of influence and p=0.05 significance contour indicated by black lines.

REFERENCES

234

235 Baker, B.H., and Mitchell, J.G., 1976, Volcanic stratigraphy and geochronology of the Kedong-236 Olorgesailie area and the evolution of the south Kenya Rift Valley: Journal of the 237 Geological Society of London, v. 132, p. 467–484. 238 Bau, M., Möller, P., and Dulski, P., 1997, Yttrium and lanthanides in eastern Mediterranean 239 seawater and their fractionation during redox-cycling: Marine Chemistry, v. 56, p. 123-240 131. 241 Berger, A., and Loutre, 1994, Precession, eccentricity, obliquity, insolation and paleoclimates, in Duplessy, J.-C., and Spyridakis, M.-T., eds., Long-Term Climatic Variations: NATO 242 243 ASI Series, v. 122, p. 107-151. 244 Buatois, L.A., Renaut, R.W., Owen, R.B., Behrensmeyer, A.K., and Scott, J.J., 2020, Animal 245 bioturbation preserved in Pleistocene magadiite at Lake Magadi, Kenya Rift Valley, and 246 its implications for the depositional environment of bedded magadiite: Scientific 247 Reports, v. 10: 6794, Doi: 10.1038/s41598-020-63505-7. 248 Campisano, C.J., Cohen, A.S., Arrowsmith, J.R., Asrat, A., Behrensmeyer, A.K., Brown, E.T., 249 Deino, A.L., Deocampo, D.M., Feibel, C.S., Kingston, J.D., Lamb, H.F., Lowenstein, 250 T.K., Noren, A., Olago, D.O., Owen, R.B., Pelletier, J.D., Potts, R, Reed, K.E., Renaut, 251 R.W., Russell, J.M., Russell, J.L., Schäbitz, F., Stone, J.R., Trauth, M.H., Wynn, J.G., 2017, The Hominin Sites and Paleolakes Drilling Project: Acquiring High-Resolution 252 253 Paleoclimate Records from the East African Rift System and Their Implications for 254 Understanding the Environmental Context of Hominin Evolution: PaleoAnthropology v. 255 2017, p. 1–43.

256 Cohen, A.S., Campisano, C., Arrowsmith, R., Behrensmeyer, A.K., Deino, A., Feibel, C., Hill, 257 A., Johnson, R., Kingson, J., Lamb, H., Lowenstein, T., Noren, A., Olago, D., Owen, R.B., Potts, R., Reed, K., Renaut, R., Schabitz, F., Tiercelin, J.-J., Trauth, M.H., Wynn, 258 259 J., Ivory, S., Brady, K., O'Grady, R., Rodysill, J., Githiri, J., Russell, J., Foerster, V., 260 Dommain, R., Rucina, S., Deocampo, D., Russell, J., Billingsley, A., Beck, C., 261 Dorenbeck, G., Dullo, L., Feary, D., Garello, D., Gromig, R., Johnson, T., Junginger, A., 262 Karanja, M., Kimburi, E., Mbuthia, A., McCartney, T., McNulty, E., Muiruri, V., 263 Nambiro, E., Negash, E.W., Njagi, D., Wilson, J.N., Rabideaux, N., Rabu, T., Sier, M.J., Smith, P., Urban, J., Warren, M., Yadeta, M., Yost, C., Zinaye, B., 2016, The 264 Hominin Sites and Paleolakes Drilling Project: Inferring the Environmental Context of 265 266 Human Evolution from Eastern African Rift Lake Deposits: Scientific Drilling, v. 21, p. 267 1-16.268 De Cort, G., Mees, F., Renaut, R.W., Sinnesael, M., Van der Meeren, T., Goderis, S., Keppens, 269 E., Mbuthia, A., and Verschuren, D., 2019, Late-Holocene sedimentation and sodium 270 carbonate deposition in hypersaline, alkaline Nasikie Engida, southern Kenya Rift 271 Valley: Journal of Paleolimnology, v. 62, p. 279-300, Doi: 10.1007/s10933-019-00092-2 272 273 Degens, E.T., and Kulbicki, G., 1973, Hydrothermal origin of metals in some East African Rift 274 Lakes. Mineralium Deposita, v. 8, p. 388-404. 275 Deocampo, D.M. and Jones, B.F., 2014, Geochemistry of saline lakes, in Drever, J.I., ed., 276 Treatise on Geochemistry 2nd Edition: Surface and Groundwater, Weathering, and Soils: Elsevier, v. 7, p. 437-469. 277

278	Deocampo, D.M., Behrensmeyer, A.K., and Potts, R., 2010, Ultrafine clay minerals of the
279	Pleistocene Olorgesailie Formation, southern Kenya Rift: diagenesis and
280	paleoenvironments of early hominins: Clays and Clay Minerals, v. 58, p. 293-309.
281	Domagalski, J.L., Eugster, H.P., and Jones, B.F., 1990, Trace metal geochemistry of Walker,
282	Mono, and Great Salt Lakes, in Spencer, R.J. and Chou, I.M., eds., Fluid-Mineral
283	Interactions: A Tribute to H.P. Eugster, Special Pub. 2: Geochemical Society, San
284	Antonio, TX, p. 315-354.
285	Emeis, K., Sakamoto, T. Wehausen, R., Brumsack, H.J., 2000, The sapropel record of the eastern
286	Mediterranean Sea – results of Ocean Drilling Program Leg 160: Palaeogeography,
287	Palaeoclimatology, Palaeoecology v. 158, p. 371-395.
288	Eugster, H.P., 1967, Hydrous sodium silicates from Lake Magadi, Kenya: Precursors of bedded
289	chert: Science, v. 157, p. 1177.
290	Foerster, V., Deocampo, D.M., Asrat, A., Gunter, C., Junginger, A., Kraemer, H., Stroncik, N.A.,
291	and Trauth, M.H., 2018, Towards an understanding of climate proxy formation in the
292	Chew Bahir basin, southern Ethiopian Rift: Palaeogeography, Palaeoclimatology,
293	Palaeoecology, v. 501, p. 111-123, Doi: 10.1016/j.palaeo.2018.04.009
294	Hillaire-Marcel, C., and Casanova, J., 1987, Isotopic hydrology and paleohydrology of the
295	Magadi (Kenya) – Natron (Tanzania) basin during the Late Quaternary:
296	Palaeogeography, Palaeoclimatology, Palaeoecology, v. 58 p. 155-181.
297	Hu, Z., and Qi, L., 2014, Sample Digestion Methods, in McDonough, W.F., ed., Treatise on
298	Geochemistry 2nd Edition: Analytical Geochemistry/Inorganic Instrumental Analysis:
299	Elsevier, v. 15, p. 87-109.

300 Ivory, S.J., Blome, M.W., King, J.W., McGlue, M.M., Cole, J.E., and Cohen, A.S., 2016, 301 Environmental change explains cichlid adaptive radiation at Lake Malawi over the past 302 1.2 million years: Proceedings of the National Academy of Sciences, v. 113, p. 11895-303 11900, doi: 10.1073/pnas.1611028113 304 Jones, B.F., Eugster, H.P., and Rettig, S.L., 1977, Hydrochemistry of the Lake Magadi Basin 305 Kenya: Geochimica et Cosmochemica Acta, v. 41, p. 53-72. 306 Konijnendijk, T.Y.M., Ziegler, M., and Lourens, L.J., 2014, Chronological constraints on 307 Pleistocene sapropel depositions from high-resolution geochemical records of ODP Sites 308 967 and 968: Newsletters on Stratigraphy, v. 47, p. 263-282, Doi: 10.1127/0078-309 0421/2014/0047 310 Laskar, J., Robutel, P., Joutel, F., Gastineau, M., Correia, A.C.M., and Levrard, B., 2004, A 311 long-term numerical solution for the insolation quantities of the Earth: Astronomy & 312 Astrophysics, v. 428, p. 261-285. 313 Leet, K., Lowenstein, T.K., Renaut, R.W., Owen, R.B., and Cohen, A., 2021, Labyrinth patterns 314 in Magadi (Kenya) cherts: Evidence for early formation from siliceous gels. Geology, 315 doi:10.1130/G48771.1 316 Lyons, R.P., Scholz, C.A., Cohen, A.S., King, J.W., Brown, E.T., Ivory, S.J., Johnson, T.C., 317 Deino, A.L., Reinthal, P.N., Mcglue, M.M., Blome, M.W., 2015, Continuous 1.3-318 million-year record of East African hydroclimate, and implications for patterns of 319 evolution and biodiversity: Proceedings of the National Academy of Science, v. 112, p. 320 15568-15573. 321 Muiruri, V.M., Owen, R.B., Lowenstein, T.K., Renaut, R.W., Marchant, R., Rucina, S.M., 322 Cohen, A., Deino, A.L., Sier, M.J., Luo, S., Leet, K., Campisano, C., Rabideaux, N.M.,

323	Deocampo, D., Shen, CC., Mbuthia, A., Davis, B.C., Aldossari, W., and Wang, C.,
324	2021, A million year vegetation history and paleoenvironmental record from the Lake
325	Magadi Basin, Kenya Rift Valley: Palaeogeography, Palaeoclimatology, Palaeoecology,
326	v. 567, 110247. Doi: 10.1016/j.palaeo.2021.110247
327	Owen, R.B., Potts, R., Behrensmeyer, A.K., Ditchfield, P., 2008, Diatomaceous sediments and
328	environmental change in the Pleistocene Olorgesailie Formation, southern Kenya Rift
329	Valley: Palaeogeography, Palaeoclimatology, Palaeoecology, v. 269, p. 17-37.
330	Owen, R.B., Muiruri, V.M., Lowenstein, T.K., Renaut, R.W., Rabideaux, N., Luo, S., Deino,
331	A.L., Sier, M.J., Deupont-Nivet, G., McNulty, E.P., Leet, K., Cohen, A., Campisano, C.
332	Deocampo, D., Shen, CC., Billingsley, A., and Mbuthia, A., 2018a, Progressive
333	aridification in East Africa over the last half million years and implications for human
334	evolution: Proceedings of the National Academy of Sciences, v. 115, p. 11174-11179,
335	doi: 10.1073/pnas.1801357115
336	Owen, R.B., Renaut, R.W., and Lowenstein, T.K., 2018b, Spatial and temporal geochemical
337	variability in lacustrine sedimentation in the East African Rift System: Evidence from
338	the Kenya Rift and regional analyses: Sedimentology, v. 65, p. 1697-1730, Doi:
339	10.1111/sed.12443.
340	Owen, R.B., Renaut, R.W., Muiruri, V.M., Rabideaux, N.M., Lowenstein, T.K., McNulty, E.P.,
341	Leet, K., Deocampo, D., Luo, S., Deino, A.L., Cohen, A., Sier, M.J., Campisano, C.,
342	Shen, CC., Billingsley, A., Mbuthia, A., Stockhecke, M., 2019, Quaternary history of
343	the Lake Magadi Basin, southern Kenya Rift: Tectonic and climatic controls:
344	Palaeogeography, Palaeoclimatology, Palaeoecology, v. 518, p. 97-118.

345	Potts, R., 2013, Hominin evolution in settings of strong environmental variability: Quaternary
346	Science Reviews, v. 73, p. 1-13.
347	Potts, R., and Faith, J.T., 2015, Alternating high and low climate variability: The context of
348	natural selection and speciation in Plio-Pleistocene hominin evolution: Journal of
349	Human Evolution, v.87, p. 5–20.
350	Potts, R., Behrensmeyer, A.K., Faith, J.T., Tryon, C.A., Brooks, A.S., Yellen, J.E., Deino, A.L.,
351	Kinyanjui, R., Clark, J.B., Haradon, C., Levin, N.E., Meijer, H.J.M., Veatch, E.G.,
352	Owen, R.B., Renaut, R.W., 2018, Environmental dynamics during the onset of the
353	Middle Stone Age in eastern Africa: Science, v. 360, p. 86–90.
354	Potts, R., Dommain, R., Moerman, J.W., Behrensmeyer, A.K., Deino, A.L., Beverly, E.J.,
355	Brown, E.T., Deocampo, D. Kinyanjui, R., Lupien, R., Owen, R.B., Rabideaux, N.,
356	Riedl, S., Russell, J.M., Stockhecke, M., deMenocal, P., Tyler Faith, J., Garcin, Y.,
357	Noren, A., Scott, J.J., Western, D., Bright J., Clark, J.B., Cohen, A.S., Heil, C.W.,
358	Keller, C.B., King, J., Levin, N.E., Shannon, K.B., Muiruri, V., Renaut, R., Rucina,
359	S.M, Uno, K., 2020, Increased ecological resource variability during a critical transition
360	in hominin evolution: Science Advances, v. 6, eabc8975. DOI: 10.1126/sciadv.abc8975
361	Rabideaux, N.M., 2018, Late Quaternary East African Environmental Change based on
362	Mineralogical and Geochemical Analysis of Outcrop and Core Material from the
363	Southern Kenya Rift. Ph.D. Dissertation, Georgia State University,
364	https://scholarworks.gsu.edu/chemistry_diss/145
365	Talling, J.F., 1992, Environmental regulation in African shallow lakes and wetlands: Revue
366	d'hydrobiologie tropicale, v. 25, p. 87-144.

Thiam, A., Jezequel, D., Groleau, A., Prevot, F., Lopes, F., Alberic, P., Quiblier, C., Bura-Nakic,
E., Ciglenecki, I, Lazar, H., and Viollier, R., 2014, Biogeochemical dynamics of
molybdenum in a crater lake: Seasonal impact and long-term removal: Journal of Water
Resources and Protection, v. 6, p. 256-271.
Vorlicek, T.-P., Kahn, M.-D., Kasuya, Y., and Helz, G.-R., 2004, Capture of molybdenum in
pyrite-forming sediments: role of ligand-induced reduction by polysulfides: Geochimica
et Cosmochimica Acta: v. 68, p. 547-556.

Core HSPDP-MAG14-2A

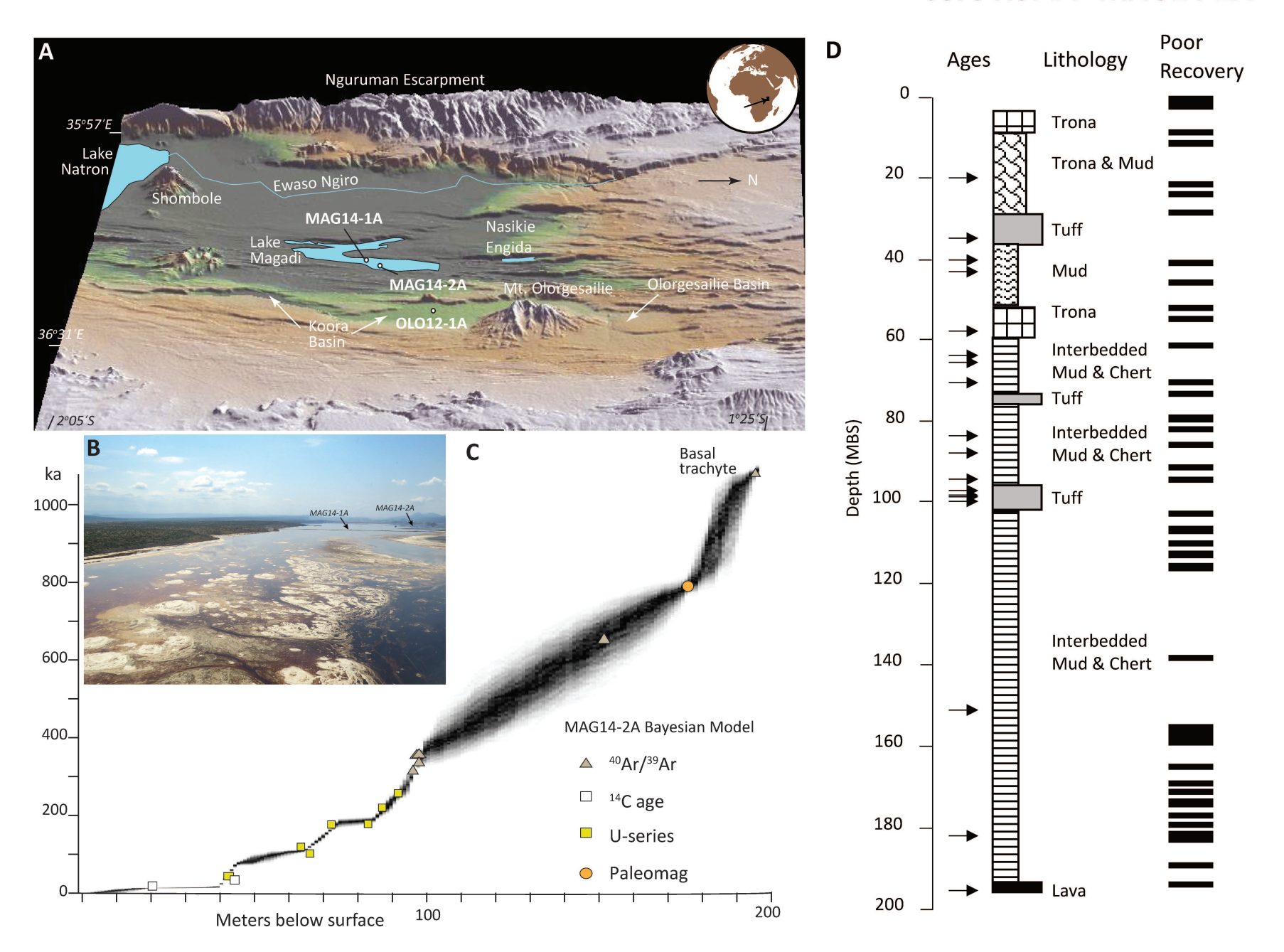


Figure 2 Deocampo et al.

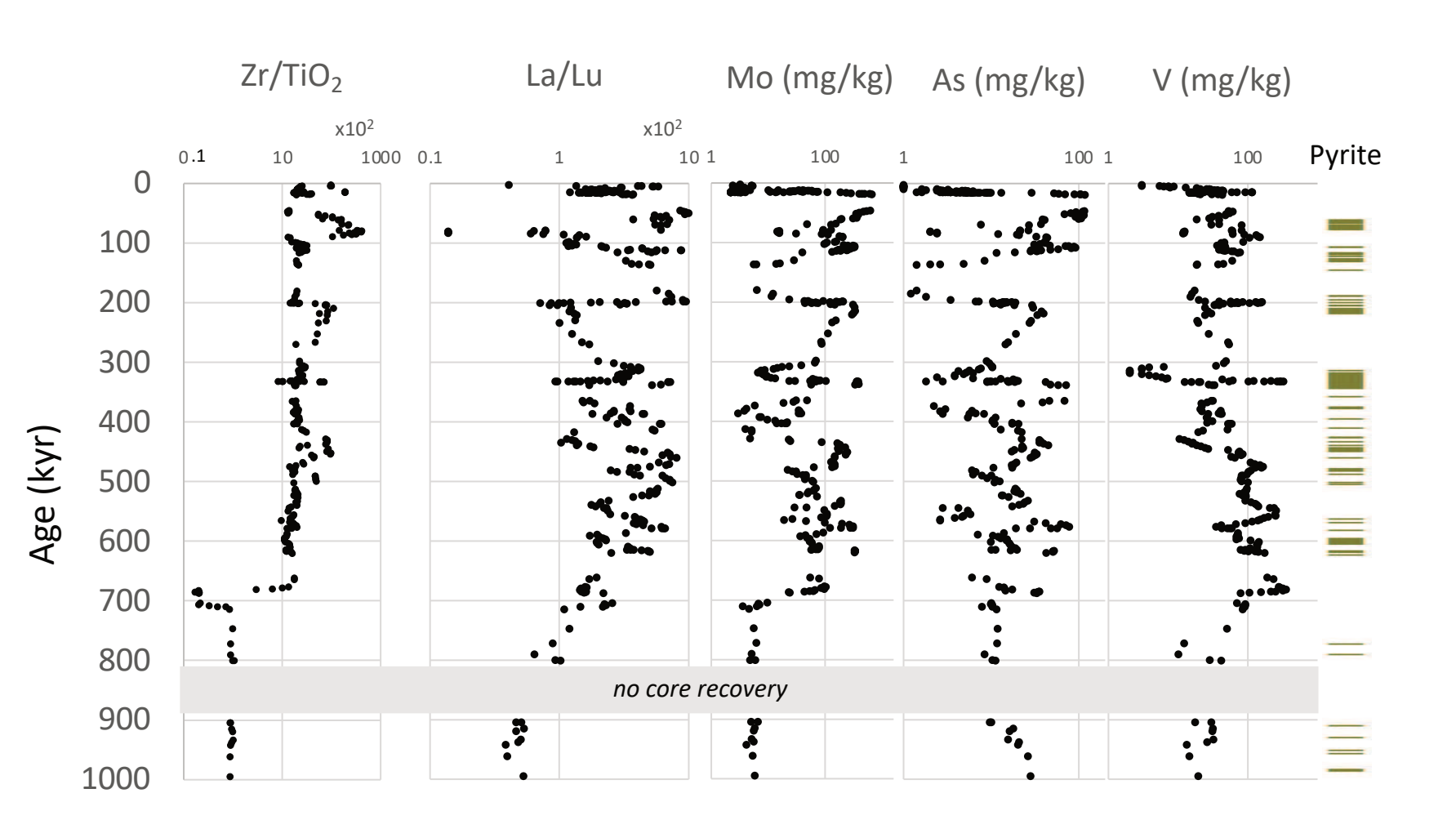


Figure 3 Deocampo et al.

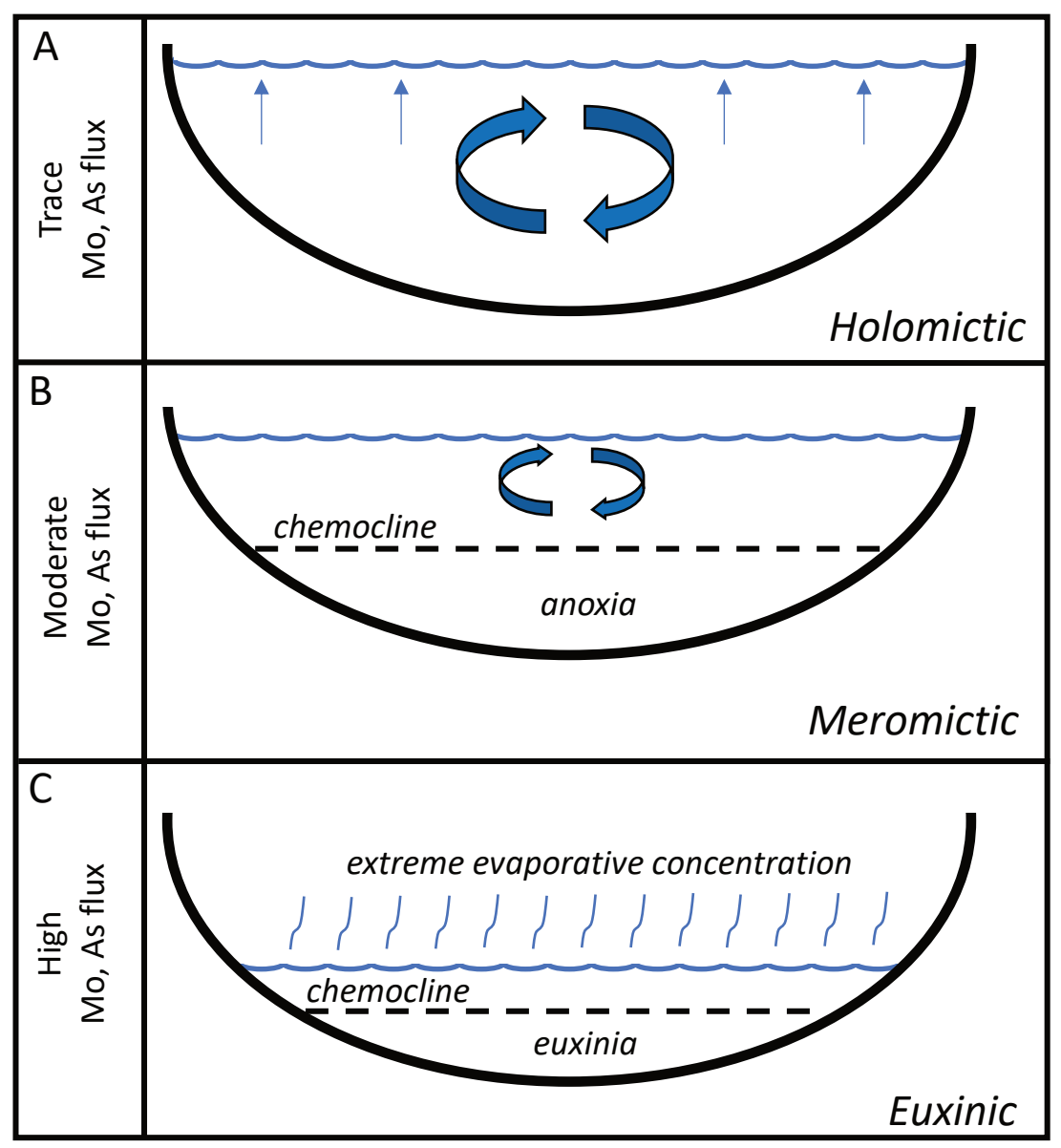


Figure 4 Deocampo et al.

